

SUPPLEMENTAL FIGURES

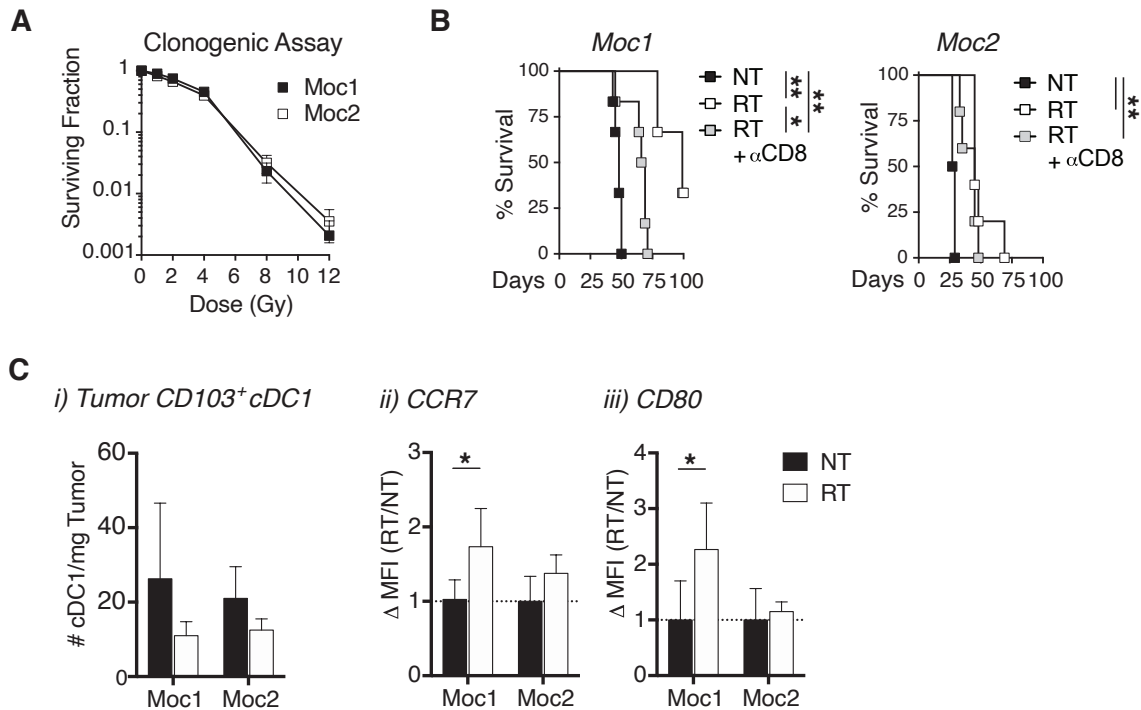


Figure S1: Radiation induces cDC1 maturation in radio-immunogenic Moc1 tumors. (A) Moc1 and Moc2 tumor cells lines were treated as described in fig 1A to quantify surviving fraction of cells at indicated doses of radiation *in vitro*. (B) Moc1 and Moc2 tumor bearing mice were treated with 12Gy of RT when tumors were ~5mm in diameter. CD8⁺ T cells were depleted and animal survival was monitored. (C) i) Tumors were harvested 3 days following radiation and the number of intratumoral CD103⁺ cDC1s per mg of tumor tissue were quantified. The MFI for ii) CCR7, and iii) CD80 was quantified on CD103⁺ cDC1 and this value was normalized to the average of the untreated controls to determine the fold change in expression following treatment. n = 4-7 animals/group. Data represent the mean \pm SD of each group. * $p < 0.05$, ** $p < 0.01$.

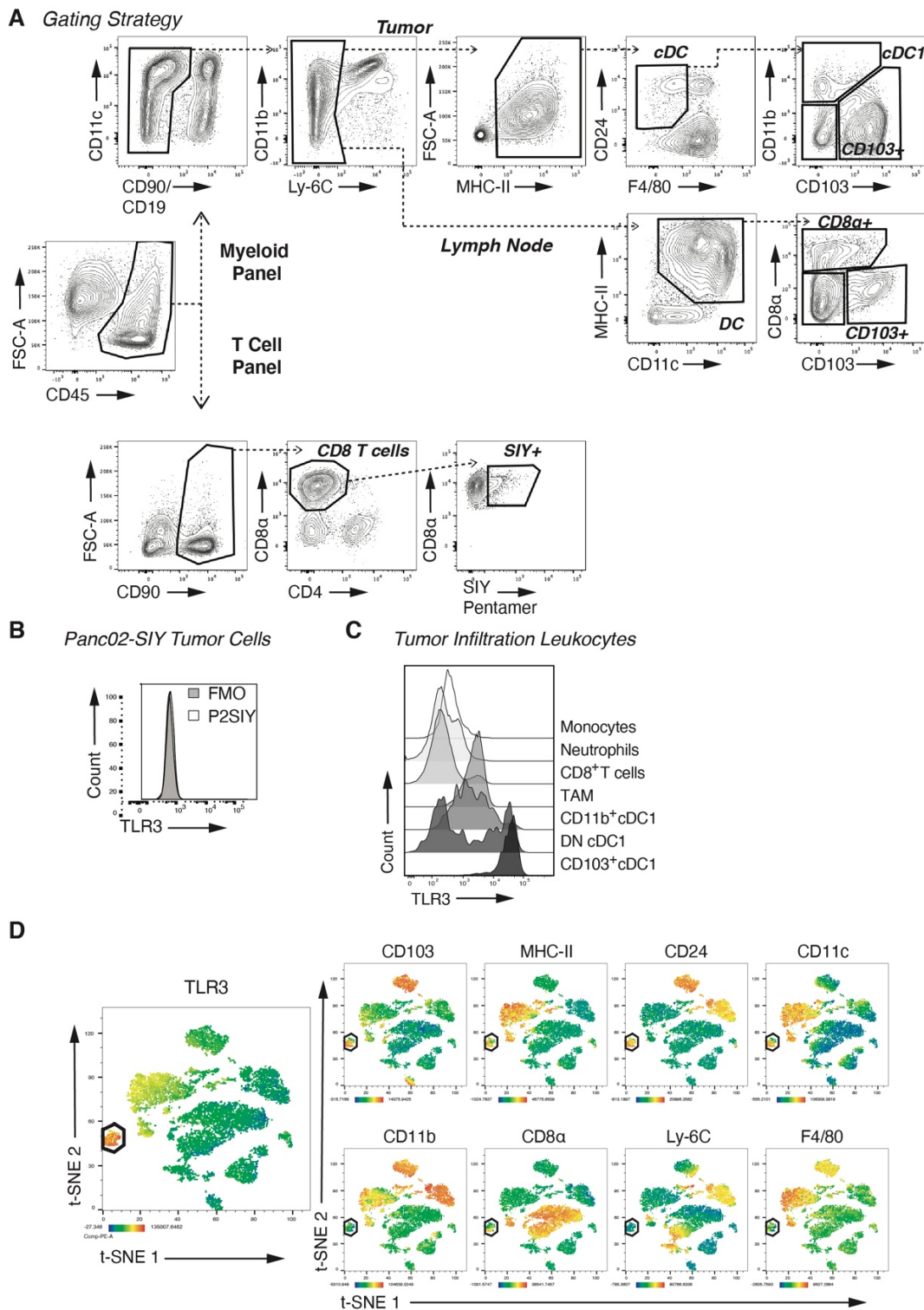


Figure S2: Gating strategy for flow cytometry analysis and TLR3 expression across cell types in the tumor. (A) Representative gating strategy from single cell suspension that begins after leukocytes were gated and doublets were removed in FlowJo. (B) Expression of TLR3 in P2SIY tumors compared to fluorescence minus one (FMO) control. (C) Expression of TLR3 within tumor infiltrating leukocyte populations (CD45⁺). (D) Dimensionality reduction of flow cytometry data using t-SNE algorithm to identify clusters of immune cells (CD45⁺) expressing TLR3 from P2SIY tumors with CD103⁺ cDC1s identified in each panel by solid black hexagon.

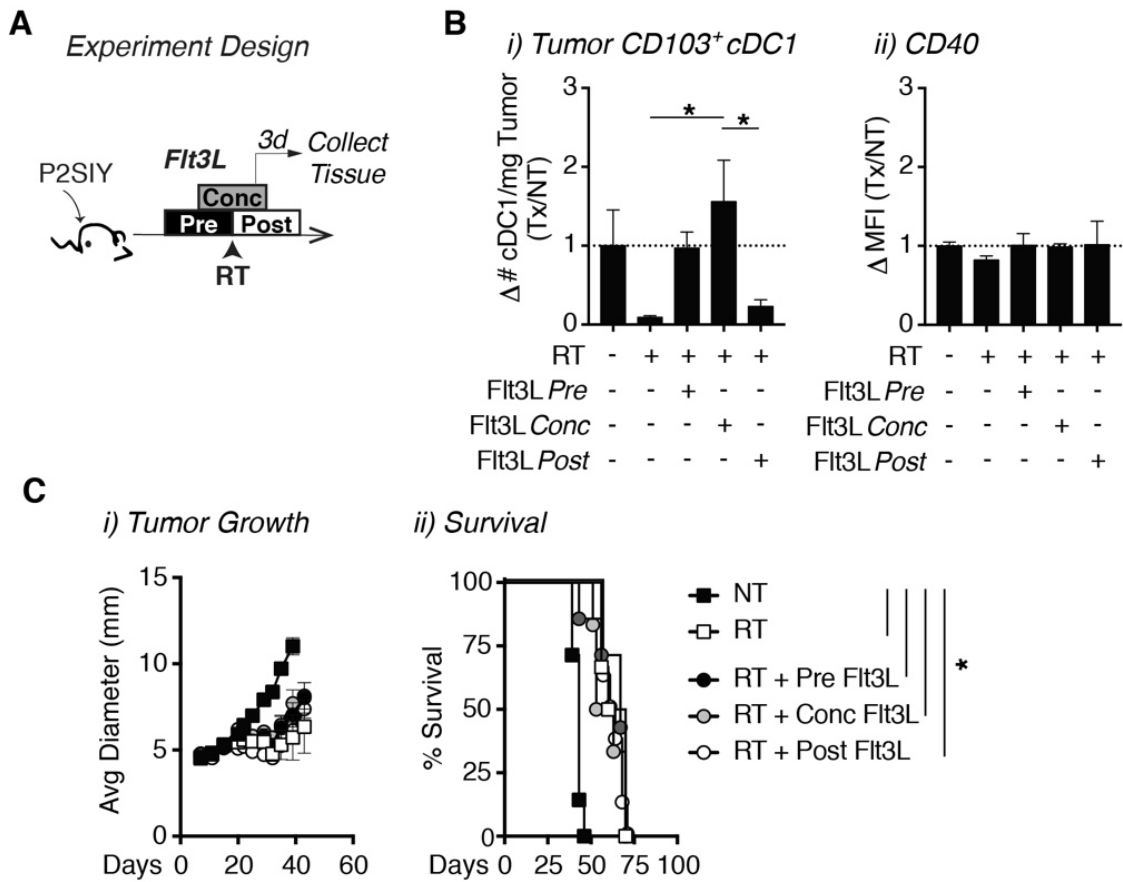


Figure S3: Increased accumulations of intratumoral cDC1s fails to improve the efficacy of radiation. (A) Experiment setup for B-C. P2SIY tumor bearing mice were treated with 9 consecutive, daily doses of Flt3L starting either prior to RT (Pre), concurrently with RT (Conc) or after treatment with RT (Post). Tissue was collected 3 days following treatment with 12Gy RT for phenotypic analysis. (B) The number of i) CD103⁺ cDC1 per mg of tumor tissue and ii) CD40 MFI on CD103⁺ cDC1s was quantified and normalized to the average value for untreated controls to calculate fold change following treatment. (C) i) Tumor growth curves and ii) animal survival after treatment with radiation and Flt3L. n = 5-8 animals/group. Data represent the mean ± SD of each group. Results shown are representative of two independent experiments. **p* < 0.05.

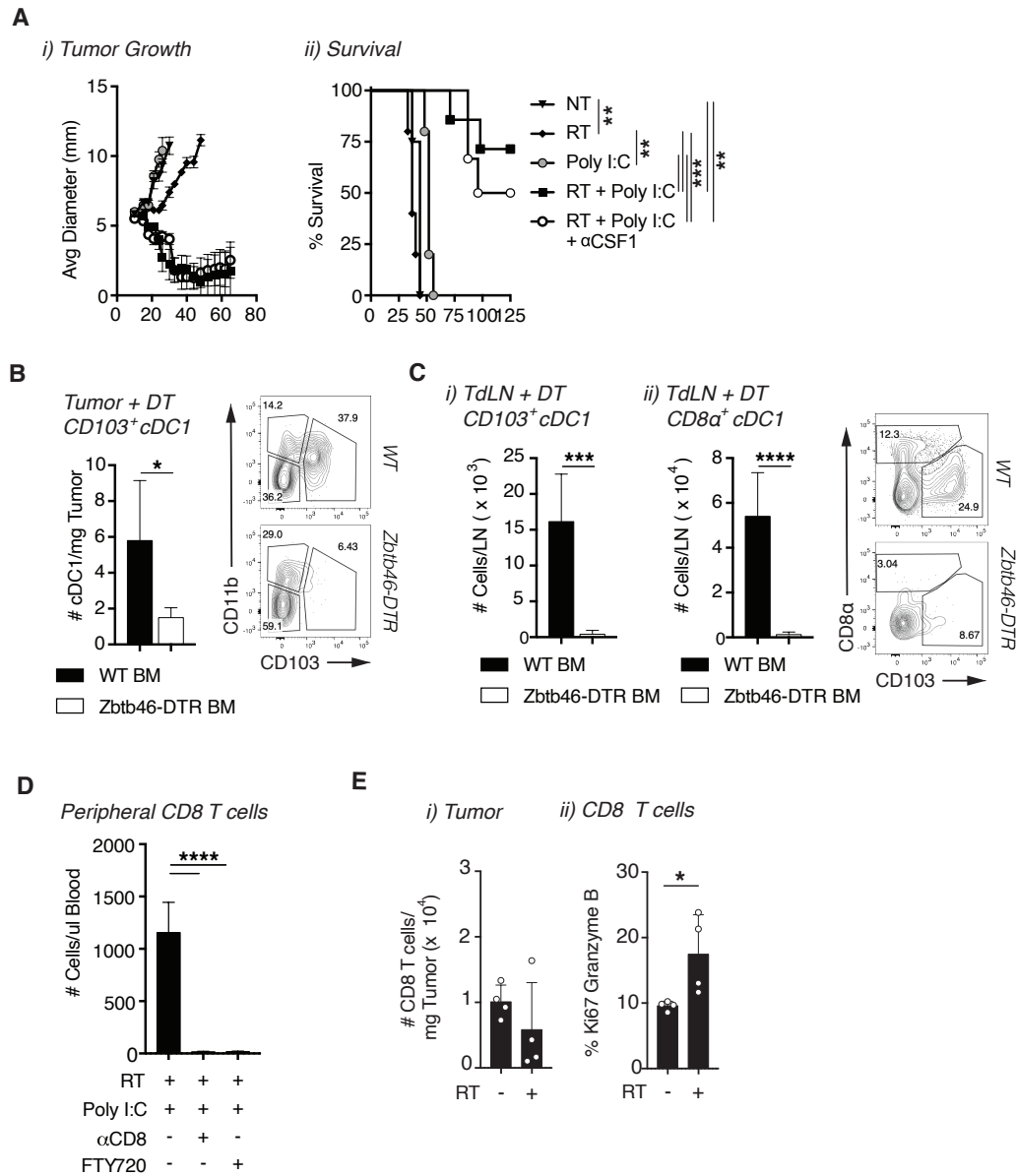


Figure S4: The role of individual immune cell subsets in the efficacy of radiation and poly I:C.

(A) P2SIY tumor bearing mice were treated with anti-CSF1 antibodies during treatment with 12Gy radiation and poly I:C. i) Tumor growth curves and ii) animal survival after treatment. **(B)** P2SIY tumors were harvested from wild-type (WT) C57BL/6 or Zbtb46-DTR bone marrow (BM) chimeras with no treatment or treatment with diphtheria toxin (DT) in addition to radiation and poly I:C. The number of intratumoral CD103⁺ cDCs/mg of tissue was quantified. **(C)** i) The number of migratory CD103⁺ cDC1s/dLN and ii) resident CD8 α ⁺ cDC1s/dLN was quantified. **(D)** Blood was collected 1 day following radiation and poly I:C in P2SIY tumors after administering FTY720 or CD8 depleting antibodies. The number of CD8⁺ T cells/ μ L of blood was quantified. **(E)** MC38 tumors were harvested 7 days following treatment with radiation and poly I:C. The number of i) CD8⁺ T cells/mg of tumor and ii) the percentage of CD8⁺ T cells co-expressing Ki67⁺ and Granzyme B⁺ was quantified. n = 4-7 animals/group. Data represent the mean \pm SD of each group. * $p < 0.05$, ** $p < 0.01$, *** $p < 0.001$, **** $p < 0.0001$.